


# Hippocampal, basal ganglia and olfactory connectivity contribute to cognitive impairments in Parkinson's disease

Korey P. Wylie<sup>1</sup>  | Benzi M. Kluger<sup>2</sup> | Luis D. Medina<sup>3</sup> |  
Samantha K. Holden<sup>4</sup> | Eugene Kronberg<sup>1,4</sup> | Jason R. Tregellas<sup>1,5</sup> |  
Isabelle Buard<sup>4</sup>

<sup>1</sup>Department of Psychiatry, University of Colorado School of Medicine, Aurora, Colorado, USA

<sup>2</sup>Department of Neurology, University of Rochester Medical Center, Rochester, New York, USA

<sup>3</sup>Department of Psychology, University of Houston, Houston, Texas, USA

<sup>4</sup>Department of Neurology, University of Colorado School of Medicine, Aurora, Colorado, USA

<sup>5</sup>Research Service, Rocky Mountain Regional VA Medical Center, Aurora, Colorado, USA

## Correspondence

Korey P. Wylie, Anschutz Medical  
Campus, Anschutz Health Sciences Bldg.,  
Mail Stop F546, 13001 East 17th Place,  
Aurora, CO 80045, USA.  
Email: [korey.wylie@cuanschutz.edu](mailto:korey.wylie@cuanschutz.edu)

## Funding information

National Institutes of Health,  
Grant/Award Numbers:  
1K02NS080885-01A1,  
1R21NS093266-01A1, K01 AT009894-01;  
Michael J. Fox Foundation for Parkinson's  
Research, Grant/Award Number: 10879

Edited by: Yoland Smith

## Abstract

Cognitive impairment is increasingly recognized as a characteristic feature of Parkinson's disease (PD), yet relatively little is known about its underlying neurobiology. Previous investigations suggest that dementia in PD is associated with subcortical atrophy, but similar studies in PD with mild cognitive impairment have been mixed. Variability in cognitive phenotypes and diversity of PD symptoms suggest that a common neuropathological origin results in a multitude of impacts within the brain. These direct and indirect impacts of disease pathology can be investigated using network analysis. Functional connectivity, for instance, may be more sensitive than atrophy to decline in specific cognitive domains in the PD population. Fifty-eight participants with PD underwent a neuropsychological test battery and scanning with structural and resting state functional MRI in a comprehensive whole-brain association analysis. To investigate atrophy as a potential marker of impairment, structural gray matter atrophy was associated with cognitive scores in each cognitive domain using voxel-based morphometry. To investigate connectivity, large-scale networks were correlated with voxel time series and associated with cognitive scores using distance covariance. Structural atrophy was not associated with any cognitive domain, with the exception of visuospatial measures in

**Abbreviations:** Assoc, association network; aTempPolar, anterior temporopolar network; BNT, Boston Naming Test; BTA, Brief Test of Attention; CDT, cluster-defining threshold; CSF, cerebral spinal fluid; CVLT-II, California Verbal Learning Test 2nd Edition; DAN, dorsal attention network; dCov, distance covariance; dlPFC, dorsolateral prefrontal cortex; DRS-2, Mattis Dementia Rating Scale 2; FAS, Verbal Phonemic Fluency; ICA, independent components analysis; ICN, intrinsic connectivity network; JLO, judgment of line orientation; lat, lateral; med, medial; MNI, Montreal Neurological Institute; MoCA, Montreal cognitive assessment; PCA, principal components analysis; PDD, Parkinson's disease dementia; PD-MCI, Parkinson's disease with mild cognitive impairment; PrC, precuneus; rs-fMRI, resting state functional magnetic resonance imaging; SDMT, symbol digits modality test; SM, somatomotor network; TMT, trail making test.

primary sensory and motor cortices. In contrast, functional connectivity was associated with attention, executive function, language, learning and memory, visuospatial, and global cognition in the bilateral hippocampus, left putamen, olfactory cortex, and bilateral anterior temporal poles. These preliminary results suggest that cognitive domain-specific networks in PD are distinct from each other and could provide a network signature for different cognitive phenotypes.

#### KEYWORDS

distance covariance, fMRI, ICA, independent components analysis, resting state

## 1 | INTRODUCTION

Parkinson's disease (PD) is a progressive neurodegenerative disorder characterized by the cardinal motor symptoms of bradykinesia, rigidity, and tremor (Christopher & Strafella, 2013; Kehagia et al., 2010). The pathological hallmark of PD is progressive neuronal cell loss and the presence of aggregated alpha-synuclein proteins in subcortical and cortical structures, termed Lewy bodies and Lewy neurites. This pathology is proposed to initially occur in the olfactory bulb and dorsal motor nucleus of the vagus nerve, subsequently spreading to the substantia nigra when motor symptoms begin to appear (Braak et al., 2003; Goedert et al., 2013). As the disease progresses, synuclein inclusions further spread to medial temporal limbic structures, such as the hippocampus and amygdala, and to the neocortex in the final stages of the disease (Stefanis, 2012). In addition to synuclein pathology, PD is also associated with Alzheimer-type amyloid plaques and neurofibrillary tangles, including in the hippocampus (Emre, 2003b; Kalaitzakis & Pearce, 2009).

Similar to Alzheimer's disease, PD is associated with cognitive decline and dementia. At diagnosis of PD, 15–20% of patients have mild cognitive impairment (PD-MCI; Aarsland, 2016). Subsequently, in the next 3 to 5 years, 20–57% of patients will experience cognitive deficits (Hanagasi et al., 2017; Kehagia et al., 2010). PD-MCI is predictive of PD dementia (PDD), which develops in up to 80% of patients with PD-MCI (Dirnberger & Jahanshahi, 2013; Hanagasi et al., 2017). As advances in treatment for PD prolong the lives of people with the disease, the incidence and prevalence of PDD may increase. Given the adverse effects on quality of life and disease burden associated with cognitive impairment, there is burgeoning interest in these non-motor symptoms of PD (Kalaitzakis & Pearce, 2009). The Movement Disorders Society Task force has developed specific clinical diagnostic criteria for PD-MCI (Litvan et al., 2012) and for PDD

(Emre et al., 2007). While such criteria provide a thorough distinction between cognitive states, they require comprehensive neuropsychological testing sessions which are initiated by the referring neurologist when concerns about cognitive decline are expressed. Identifying risk to cognitive decline before its manifestation may be therefore a new strategy. Early identification might be especially important for potential early intervention strategies targeting modifiable cognitive risk factors, such as vascular risk (Raz & Rodrigue, 2006).

In recent years, there has been an increasing focus on finding a biomarker to quantify the risk of cognitive impairment in PD, as well as to develop effective pharmacological interventions (Delgado-Alvarado et al., 2016; Hohenfeld et al., 2018). Neuroimaging biomarkers, in particular, may be promising due to their non-invasive nature and ability to detect the specific neuronal pathology contributing to dementia, in terms of the contributions of individual neuroanatomical regions. Several studies have found hippocampal atrophy to be associated with PDD (reviewed in Delgado-Alvarado et al., 2016). However, this finding is not universal and may not be as prominent in the early stages of cognitive decline (Christopher & Strafella, 2013). In addition, while impairments in executive function, attention, and visuospatial abilities rather than amnesic deficits are commonly found during early stages of cognitive decline in PD, some subgroups of patients may instead exhibit greater difficulties with memory and language (Emre, 2003b). This heterogeneity in cognitive profiles may benefit from multimodal identification, including self-reports, clinical evaluation, neuropsychological testing, and possibly neuroimaging and neurophysiological assessments, in order to better characterize cognitive phenotypes.

A rising idea suggests that connectivity biomarkers of early disease pathology may be more sensitive than gray matter atrophy (Amboni et al., 2015; Seibert et al., 2012). Connectivity measured using resting state functional

magnetic resonance imaging (rs-fMRI) is particularly attractive for clinical populations, because it does not require cognitively demanding tasks or active effort and can be applied to patients in a wide variety of conscious and cognitive states. However, previous rs-fMRI studies of cognition in PD have yielded mixed results (Gao & Wu, 2016; Hohenfeld et al., 2018). These studies have been limited in scope, analyzing a small number of regions or networks, selected in advance based on widely varying criteria, or lacking adequate methodology to deal with heterogeneity. Thus, by focusing on a select few connections, these studies potentially miss substantial influences on cognition from the vast number of connections within the brain. This narrowly focused and selective approach to connectivity shares the same limitations as early regionally focused neuroimaging studies, rather than the broader voxel-based whole-brain investigations that are now standard in task-based fMRI. To date, voxel-level, whole-brain data-driven investigations of connectivity and cognition in PD remain rare (Gao & Wu, 2016) but could potentially take advantage of the increased sensitivity of rs-fMRI to early stage pathology, as well as yield results more comparable to other imaging modalities and coordinate-based meta-analysis.

The current investigation applies a novel, whole-brain, data-driven analysis to examine the neural correlates of cognitive domains in the context of PD. Rather than focusing on group differences between broad subtypes such as PD-MCI or PDD, subject's scores for each cognitive domain were analyzed on continuum. The analytic approach measures voxel-level connectivity using independent components analysis (ICA) in PD subjects with a wide range of cognitive abilities. It analyzes the relationship between connectivity and cognition using distance covariance (dCov; Székely et al., 2007). Distance covariance is a recently developed statistical method, with power and flexibility equivalent to machine learning methods (Sejdinovic et al., 2013). Using the combination of ICA and dCov, we hypothesize that cognitive performance in PD will be associated with connectivity involving the basal ganglia and hippocampus, according to the proposed broader primary and progressive pathology associated with the disease (Braak et al., 2003; Goedert et al., 2013). Specifically, connectivity to these subcortical regions and relevant large-scale networks (e.g., the Dorsal Attention Network for neurocognitive tests of attention) will influence measures of executive function, attention and visuospatial processing, the cognitive domains most commonly affected in PD. Voxel-level results from this novel analysis of functional connectivity were then compared with gray matter atrophy, as measured with voxel-based morphometry (VBM). Gray matter atrophy was measured using VBM. Although surfaced-based cortical

thickness (Fischl, 2012) is arguably a more sensitive measure of atrophy for the cortical regions, it does not examine subcortical regions such as the hippocampus, nor does it allow for direct comparison with voxel-based dCov results. We expect that, in contrast to the more sensitive functional connectivity measure, gray matter atrophy in the PD brain will not be associated with any cognitive measure.

## 2 | MATERIALS AND METHODS

### 2.1 | Study population

Sixty-eight patients with PD were recruited through the University of Colorado Hospital's Movement Disorder, Memory Disorder, and Neuropsychology Clinics. Diagnosis of PD was defined using UK Brain Bank Criteria (Hughes et al., 1992). All subjects were age 40 or older and on stable medications for at least 30 days. All subjects were tested in their usual medication state (i.e., "ON"). All subjects gave informed consent to participate. The study was approved by the Colorado Multiple Institution Review Board and is in accordance with the ethical standards of the Declaration of Helsinki.

Exclusion criteria included features suggestive of other causes of parkinsonism or Parkinson-plus syndromes; features suggestive of other causes of dementia, including moderate to severe cerebrovascular disease by history or imaging; history of major head trauma; history of deep brain stimulation, ablation surgery, or other brain surgery; evidence for moderate depression based on the Hospital Anxiety Depression Scale (score > 11; Zigmond & Snaith, 1983); as well as MRI exclusion factors (claustrophobia, weight >300 lb, metal in the body). Ten subjects were subsequently excluded for excessive movement during fMRI scanning (>2 mm or 2° in any direction), because fMRI motion correction techniques are of limited benefit in these cases (Parkes et al., 2018).

Demographics and clinical characteristics for the participants that underwent fMRI scanning are listed in Table 1. A total of 58 subjects were included, with a mean age of 70 years, ranging from 55 to 92 years old, with 39 men and 19 women.

### 2.2 | Cognitive evaluation

All patients underwent a comprehensive battery of neuropsychological tests. Included in the battery was the Montreal Cognitive Assessment (MoCA), Mattis Dementia Rating Scale 2 (DRS-2), Trail Making Test (TMT) Parts A and B, Brief Test of Attention (BTA), Boston Naming

TABLE 1 Patient demographic, clinical and cognitive characteristics

		Range (min:max)	Missing data (n)
Sex (M, F)	$n = 39, n = 19$		
Age	$70.42 \pm 7.94$	55:92	
Education	$16.21 \pm 2.75$		
H & Y stage	$2.71 \pm 1.05$	0:5	
UPDRS part III	$22.43 \pm 8.8$	0:43	
LEDD	$530.28 \pm 431.84$	0:2100	
MoCA	$24.52 \pm 4.26$	9:30	0
DRS-2	$132.97 \pm 12.27$	82:144	0
TMT part A	$56.27 \pm 53.96$	22.0:402.0	2
TMT part B	$159.81 \pm 128.44$	48.0:300.0	6
BTA	$11.74 \pm 8.32$	2:20	4
BNT	$55.91 \pm 3.84$	47:60	4
Verbal fluency	$34.76 \pm 16.9$	12:63	4
CVLT-II trials 1–5	$34.5 \pm 13.7$	11:69	3
CVLT-II long delay	$6.57 \pm 4.7$	0:16	3
SDMT Oral	$35.31 \pm 27.76$	15:69	3
JLO score	$25.93 \pm 5.11$	11:34	3
Attention composite	$-0.01 \pm 1.06$	-6.51:0.86	
Executive function composite	$0.03 \pm 1.02$	-5.54:1.03	
Language composite	$0.06 \pm 0.87$	-3.63:1.30	
Learning & memory composite	$0.03 \pm 1.02$	-3.08:1.93	
Global cognition composite	$0.06 \pm 0.98$	-4.00:1.20	
Visuospatial	$0.00 \pm 1.00$	-2.92:1.58	

Note: Values are mean  $\pm$  standard deviation unless otherwise indicated. Key: LEDD, levodopa equivalent daily dose; H & Y, Hoehn and Yahr stage; UDPRS-III, Unified Parkinson's Disease Rating Scale; MoCA, Montreal Cognitive Assessment; DRS-2, Dementia Rating Scale 2; TMT, Trail Making Test; BTA, Brief Test of Attention; BNT, Boston Naming Test; CVLT-II, California Verbal Learning Test 2nd Edition; SDMT, and the Symbol Digits Modality Test; JLO, Judgment of Line Orientation.

Test (BNT), Verbal Phonemic Fluency (FAS), California Verbal Learning Test 2nd Edition (CVLT-II), Judgment of Line Orientation (JLO), and the Symbol Digits Modality Test (SDMT). These tests were chosen based on previous work validating the PD-MCI diagnostic criteria (Goldman et al., 2013).

Not all patients were able to complete the full cognitive battery. Per patient's self-reports, this was typically due to mental fatigue or worsening motor symptoms. Although these symptoms likely overlap with cognitive impairment in some subjects, this is not the case for all subjects. Therefore, to avoid introducing potential estimation bias due to missing data, a multiple imputation procedure was used to infer missing cognitive scores (Buuren, 2018; Nakagawa & Freckleton, 2008). This procedure is currently accepted as the best general method to deal with incomplete data. Additionally, multiple imputation introduces less bias than

alternatives, such as surrogate scores based on a “worst-case” scenario.

Cognitive data were checked for missing observations and found to violate the assumption that data were missing completely at random (MCAR; Little's MCAR Test,  $p = 0.007$ ). Therefore, data were imputed to create five multiple imputations using Markov chain Monte Carlo (MCMC) simulation, and pooled results were used for the final analyses. None of the imputed data significantly differed from the original data (all  $p > 0.05$ ).

For data reduction purposes, and in contrast to multiple comparisons with the individual cognitive tests used, cognitive composite scores were created using principal components analysis (PCA) for each set of imputed data separately. Tests were grouped conceptually following their theoretical relation to the underlying cognitive processes they measure. Composite scores were created from the uncorrected raw scores for two tests per domain as

follows: Attention (TMT-A and BTA), Executive Function (TMT-B and SDMT Oral), Language (BNT and FAS), Learning and Memory (CVLT-II Trials 1–5 Total Learning Score and CVLT-II Long Delay Free Recall), and Global Cognition (MoCA and DRS-2 total scores). No composite score was created for the visuospatial domain, given that only one test score was available. Therefore, a sample-based *z*-score was created from JLO scores and used as a measure of visuospatial ability. Summary statistics for each individual cognitive test and composite scores are listed in Table 1.

## 2.3 | MRI acquisition

Images were acquired on a 3.0T Signa scanner (General Electric, Milwaukee), using an 8-channel head coil and a 3-D, extended dynamic range, inversion recovery SPGR ASSET parallel imaging sequence. Structural scans were acquired with the following parameters: TR = 2200 ms, TE = 2 ms, matrix = 256 × 256, voxel size = 1 × 1 mm<sup>2</sup>, slice thickness = 1 mm, flip angle = 8°. Functional scans were acquired with the following parameters: TR = 2000 ms, TE = 26 ms, matrix = 64 × 64, voxel size = 3.4 × 3.4 mm<sup>2</sup>, slice thickness = 3.5 mm, gap = 1.5 mm, interleaved, flip angle = 70°. Total resting state scanning time 10 min. MRI images were acquired within 1 day of neurocognitive testing.

## 2.4 | Structural preprocessing and VBM analysis

VBM is a common neuroimaging method used to quantify atrophy *in vivo* using structural MRI scans (Ashburner & Friston, 2000). It is a data-driven, whole-brain, and automated analytic technique, able to measure neuropathologic changes in gray matter volume at the voxel level resulting from neuropsychiatric and neurologic disorders, including PDD (Delgado-Alvarado et al., 2016).

VBM was implemented using SPM12 (<https://www.fil.ion.ucl.ac.uk/spm/software/spm12>). Subject's structural images were segmented into gray matter, white matter, and cerebrospinal fluid (CSF) using unified segmentation (Ashburner & Friston, 2005). Normalization to Montreal Neurological Institute (MNI) space was accomplished using a nonlinear DARTEL transform (Ashburner, 2007). Normalized images were then modulated to ensure that the overall amount of tissue type was not altered during spatial normalization. Finally, images were smoothed with an 8-mm full-width at half-maximum Gaussian kernel.

Associations between gray matter volume and cognitive measures were measured using a general linear model, with age, sex, education, and intracranial volume as covariates. Significance threshold was determined with a cluster-defining threshold (CDT) of  $p < 0.005$ , and a cluster-level threshold of  $p < 0.05$ , corrected by false discovery rate (FDR).

## 2.5 | Functional connectivity analysis

### 2.5.1 | Functional preprocessing

fMRI data were preprocessed using SPM12 (<https://www.fil.ion.ucl.ac.uk/spm/software/spm12>) for each subject individually. The first four images were excluded for saturation effects. Echo planar images from each subject were realigned to subject's mean volume, resliced to isotropic 3-mm voxels, normalized to the MNI template using unified segmentation (Ashburner & Friston, 2005), and smoothed with an 8-mm full-width at half-maximum Gaussian kernel.

### 2.5.2 | Independent component analysis (ICA)

Spatial ICA was carried out using GIFT v3.0b (<https://icatb.sourceforge.net>; Calhoun et al., 2001). Fifty components were estimated based on minimum description length (MDL) criteria and extracted using the infomax algorithm (Bell & Sejnowski, 1995; Li et al., 2007). Voxel time series were temporally concatenated across subjects and then variance-normalized in ICA preprocessing. Two PCA data reduction steps were used, with 70 and 50 components included after each. Resulting component spatial maps were back-reconstructed with GICA3 and scaled to *z*-scores (Erhardt et al., 2011). All spatial maps and time courses were visually inspected to identify noise components. Ten components were identified as artifacts based on spatial distributions that were primarily in CSF or white matter, or high-frequency oscillations, and were excluded from further analysis. To identify common intrinsic connectivity networks (ICNs) such as the default mode network, group mean ICA spatial maps were correlated with published ICA templates (Shirer et al., 2012; Yeo et al., 2011). ICA components without template matches were described based on anatomy (e.g., a bilateral anterior temporal lobe network). Following group ICA and template matching, whole-brain networks were back-reconstructed individually for each subject in order to investigate associations with that subject's cognitive scores.

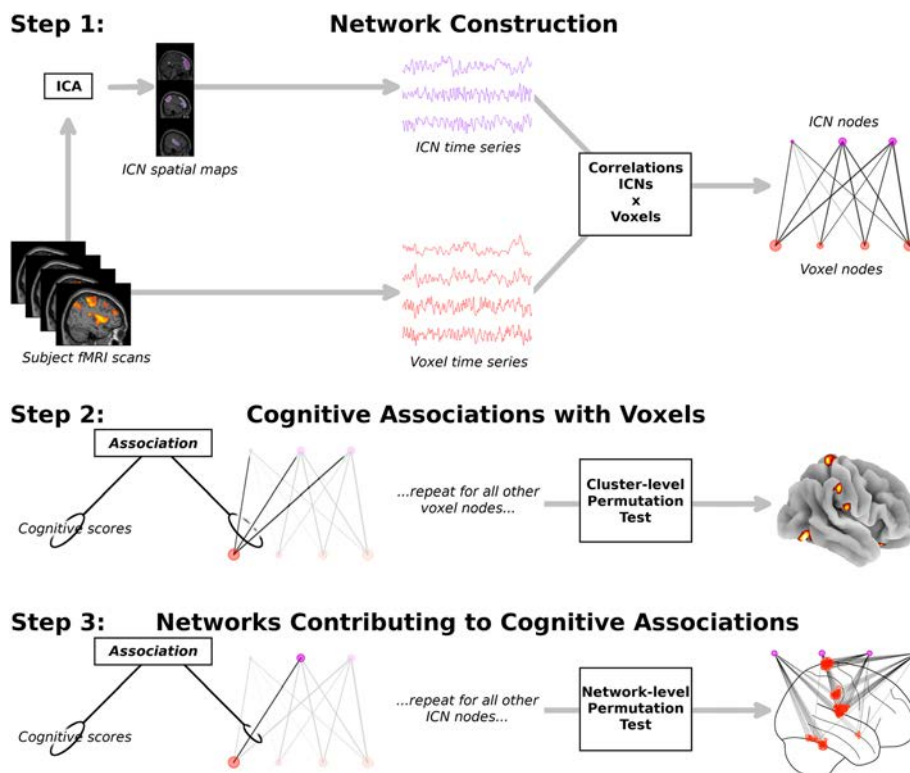


**FIGURE 1** dCov analysis overview. Step 1: Network construction. Independent components analysis (ICA) was used to estimate time series for intrinsic connectivity networks (ICNs) in subject's fMRI scans. All ICN time series were correlated with all voxel time series, resulting in a bipartite graph, with a vector of correlations representing each voxel's higher-level associations. Step 2: Cognitive associations with voxels. Distance covariance (dCov) was applied to each voxel's connectivity vector individually, resulting in a dCov test statistic for each voxel. A cluster-level permutation test was used to correct for multiple comparisons, resulting in a whole-brain volume displaying where in the brain connectivity is associated with the cognitive measure. Step 3: Networks contributing to cognitive associations. dCov was then applied to each individual connection for all voxels surviving multiple comparison correction. A network-level permutation test was used to correct for multiple comparisons. Resulting bipartite graph shows which ICNs contribute to associations between cognition and the voxels in the previous step.

### 2.5.3 | Subject-level whole-brain network construction

Next, back-reconstructed ICN time series were correlated with each voxel's time series in a functional connectivity analysis (Figure 1). The resulting vector of bivariate simple correlations for each voxel represents the set of extrinsic inputs and outputs unique to that voxel, which has been termed its "connectional fingerprint" (Passingham et al., 2002). In this context, connectivity refers to a voxel's interactions with the entire neural processing system, or large-scale networks identified with ICA, rather than its connectivity with another voxel. To calculate connectional fingerprints, nuisance signals such as CSF, white matter, and six movement parameters were regressed out of all time series. Time points with excessive movement were censored (Power et al., 2012). Following nuisance signal removal and movement control precautions, time

series for every gray matter voxel was correlated with each ICN component time series. The resulting vector of correlations, the voxel's connectional fingerprint, efficiently and comprehensively summarizes its connectivity to all regions within the brain and was subsequently tested for associations with cognitive scores, after removing the influences of age, sex, and education using linear regression residuals (Hua & Ghosh, 2015).

### 2.5.4 | Cognitive associations with voxels

Distance covariance is a recently developed multivariate technique that tests the statistical independence of two vectors with arbitrary dimensions (Székely et al., 2007). The dCov statistic is zero if and only if the random vectors are independently distributed and increasingly positive otherwise. Compared with similar techniques

(e.g., mass univariate Pearson correlations, and maximal information coefficient), dCov has demonstrated increased statistical power for identifying associations in large datasets (Simon & Tibshirani, 2014). Code used to calculate dCov in the current study are publicly available ([https://github.com/koreywyllie/Analyses\\_toolbox](https://github.com/koreywyllie/Analyses_toolbox)).

dCov analyses in the current study proceeded in two steps. First, dCov was calculated for each gray matter voxel, using each subject's connectivity vector for that voxel along with the subject's cognitive domain score (see Section 2.2) as input (Figure 1). This resulted in an unthresholded whole-brain statistical map, showing associations between voxel-level connectivity and cognitive scores. Results were thresholded and corrected for multiple comparisons using a modification of Nichol's cluster-level non-parametric test (Nichols & Holmes, 2002). Consistent with the null hypothesis of no clusters of adjacent voxels, 5000 volumes were generated by permuting subject's cognitive scores for each voxel. Empirical cumulative distribution functions (c.d.f.) were calculated for each voxel as the proportion of times the permutation dCov statistic exceeded the original dCov statistic at that voxel. For the permutation volumes, an empirical c.d.f. for all voxels were calculated in an identical manner. All volumes were then thresholded using a CDT of  $p < 0.005$ . Lastly, resulting cluster sizes were calculated. In the original (i.e., non-permutation) thresholded whole-brain statistical map, a cluster was considered significant after correcting for multiple comparisons if the permutation  $p$ -value of obtaining a cluster this size or larger was significant at  $p < 0.05$ . Significant clusters were displayed as cortical surface projections (Fischl et al., 1999) using functions provided by nilearn (<https://nilearn.github.io/>).

### 2.5.5 | Networks contributing to cognitive associations

To better understand the specific elements of the connectivity vector that contributed to each voxel's significance in the whole-brain analysis, dCov was used to test connectivity of the elements of the vector individually, using an individual scalar correlation coefficient and the scalar cognitive score as input (Figure 1). Resulting dCov statistics for each connection were thresholded and corrected for multiple comparisons using a cluster-level permutation test, similar to that used in the preceding voxel-level association analysis. First, dCov was applied to individual connections between a voxel and an ICN (Figure 1). Next, empirical c.d.f. were calculated and compared against a CDT. In contrast to the voxel-level analysis (see Section 2.5.4), however, the definitions of "cluster" and "adjacent" in the context of a network are unclear. This

discrepancy can be resolved using definitions provided by the field of graph theory. In graph theory, a connection is said to be adjacent to an ICN node if it is connected to it, for example, if an edge between nodes  $i$  and  $j$  is denoted by the ordered pair  $(i, j)$ , then it is adjacent to nodes  $i$  and  $j$  (Newman, 2010). Using this definition, a cluster is defined as a set of adjacent connections. As such, cluster size is determined as the number of connections to an individual ICN ("unweighted degree" in graph theory terminology). With this definition, cluster size was calculated and compared with the null distribution from a non-parametric permutation test. An individual connection was considered significant, after correcting for multiple comparisons, if it was located within a cluster of significant size.

In order to determine the ICNs influencing the association between cognitive scores and neuroanatomy, all significant voxels ( $p < 0.05$ , corrected) in the voxel-level association analysis were analyzed in the network-level association analysis. dCov was calculated for each connection to every ICN. Each connection was thresholded with a CDT of  $p < 0.005$ . The null distribution of the unweighted degree was calculated using 5000 permutation networks and used to correct for multiple comparisons at the network level. An individual connection was considered significant, after correcting for multiple comparisons, if the degree of its adjacent ICN node was significant at  $p < 0.05$ . Significant connections were displayed as two-dimensional sagittal, coronal, and axial projections in MNI space in the "glass brain" format, along with volumetric renderings of subcortical structures (Hammers et al., 2003).

## 3 | RESULTS

### 3.1 | Demographic, clinical and cognitive characteristics of participants

Baseline group sex differences were associated with age ( $M > F$ ,  $t = -3.1$ ,  $p = 0.003$ ), attention ( $M < F$ ,  $t = 3.1$ ,  $p = 0.004$ ), executive function ( $M < F$ ,  $t = 3.9$ ,  $p = 0.0002$ ), language ( $M < F$ ,  $t = 3.1$ ,  $p = 0.003$ ), learning and memory ( $M < F$ ,  $t = 3.2$ ,  $p = 0.002$ ), and global ( $M < F$ ,  $t = 3.4$ ,  $p = 0.001$ ) cognitive composite scores. Following removing the effects of age, sex, and education with linear regression, no significant group differences were observed ( $t = 0$  in all cases).

### 3.2 | ICA and network identification

In the functional connectivity analysis, 40 ICNs matched templates for known networks, including 14 networks

commonly identified in fMRI (Shirer et al., 2012) and several of their subnetworks. ICNs associated with cognitive domains are displayed in Figure S1, all other template-matching ICNs in Figure S2, and ICA components matching noise templates in Figure S3. The somatomotor network (SM) was subdivided into dorsal and ventral components (dSM and vSM, respectively), corresponding to spatial maps primarily centered on the body and facial representations of the sensorimotor cortex (Yeo et al., 2011), as well as left and right components (L SM and R SM, respectively), corresponding to lateralized hand representations of the sensorimotor cortex. Other ICNs corresponded to association regions for other primary sensory modalities, such as the lateral visual association network (lat Visual Assoc) encompassing bilateral occipitotemporal regions. Limbic and paralimbic networks included bilateral insulae, medial temporal (med Temporal), orbitofrontal, and anterior temporopolar (aTempPolar) networks. Higher association cortices were encompassed by ICNs centered on the right and left dorsolateral prefrontal cortices (R dlPFC and L dlPFC, respectively), and precuneus (PrC) networks. Subcortical networks included distinct ICNs encompassing putamen and caudate. These latter ICNs represent widespread activity throughout the entire bilateral putamen or caudate respectively.

### 3.3 | Associations with cognitive domains

Following ICA and network identification, each voxel's connectivity was tested for associations with cognitive composite scores from each domain using dCov in a whole-brain analysis. The analysis proceeded in two steps (Figure 1). First, the neuroanatomical regions associated with each cognitive domain were identified by examining each voxel's connectivity. Second, the specific influential ICNs contributing to each cluster identified in the previous step were identified. For each cognitive domain, this dual level analysis localized both the neuroanatomy as well as the networks influencing processing associated with that domain in PD.

### 3.4 | Attention

Attention cognitive composite scores were associated with connectivity to clusters in the right inferior gyrus, right and left middle frontal gyri, right subgenual cingulate cortex, right gyrus rectus, and left middle cingulate cortex (Figure 2, significant at cluster-level  $p < 0.05$ , corrected). Cluster sizes and locations in

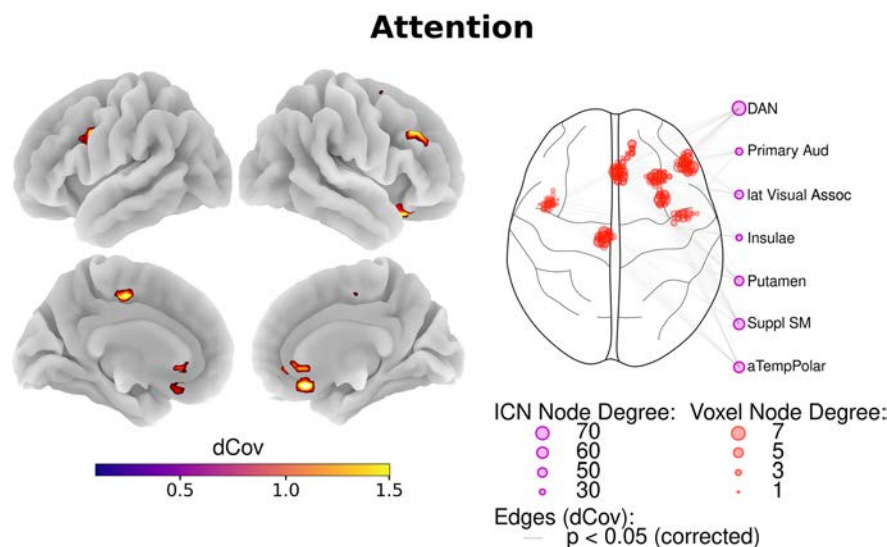


**FIGURE 2** Cortical and network associations with attention. Left: Cortical associations displayed as surface renderings. Distance covariance (dCov) was applied to each voxel's connectivity vector, followed by a cluster-level correction for multiple comparisons, resulting in clusters of voxels associated with attention cognitive composite scores. Attention was associated with connectivity to right inferior gyrus, right and left middle frontal gyri, right subgenual cingulate cortex, right gyrus rectus, and left middle cingulate cortex (all clusters  $p < 0.05$ , corrected). Right: Intrinsic connectivity networks (ICNs) influencing cortical associations. Distance covariance was then applied to the individual components of each voxel's connectivity vector, identifying connectivity with ICNs influencing associations with cognitive scores. Seven ICNs influenced associations with attention scores, including the dorsal attention (DAN), primary auditory (Primary Aud), lateral visual association (lat Visual Assoc), supplementary somatomotor (Suppl SM), and anterior temporopolar (aTempPolar) networks (all connections  $p < 0.05$ , corrected).



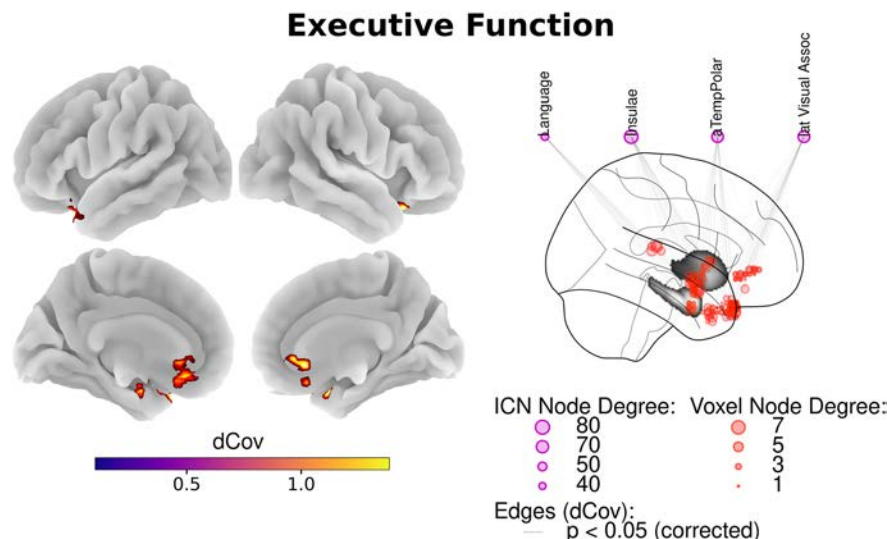


**FIGURE 3** Cortical and network associations with executive function. Left: Cortical associations displayed as surface renderings. As measured by distance covariance (dCov), executive function was associated with clusters in the left thalamus, left putamen, bilateral parahippocampal gyri, left hippocampus, bilateral anterior temporal poles, subgenual cingulate, and orbitofrontal cortices (all clusters  $p < 0.05$ , corrected). Right: Intrinsic connectivity networks (ICNs) influencing cortical associations. Four ICNs influenced associations with executive function scores, including the language, insulae, anterior temporopolar (aTempPolar), and lateral visual association (lat Visual Assoc) networks (all connections  $p < 0.05$ , corrected). Subcortical hippocampal and basal ganglia volumes are outlined in gray for visual orientation relative to position of significant voxels (red circles).

terms of MNI coordinates for all significant clusters of association are listed in Table S1. No subcortical clusters were associated with attention scores (all clusters  $p > 0.05$ , corrected). Specifically, no localized cluster of voxels within the putamen were associated with attention scores. However, as noted below, the bilateral putamen network as a whole contributed to associations with attention scores in the above clusters.

Seven networks significantly contributed to associations between attention scores and the above clusters. The Dorsal Attention Network (DAN) was the most influential, affecting associations with voxels in the right inferior frontal gyrus and subgenual anterior cingulate. Connectivity involving the bilateral putamen and aTempPolar ICNs influenced associations in the subgenual anterior cingulate and middle frontal gyri clusters bilaterally. Additional influential networks included primary and associative motor and sensory networks, such as the supplementary somatomotor (Suppl SM), lat visual assoc, primary auditory, and insulae networks (Figure 2, right, all connections significant at  $p < 0.05$ , corrected).

In contrast to the functional connectivity associations, gray matter volume was not associated with attention cognitive composite scores in the VBM analysis (all clusters  $p > 0.05$ , corrected).

### 3.5 | Executive function

Executive function composite scores were primarily associated with connectivity involving subcortical and paralimbic clusters. These included clusters in the left thalamus, left putamen, bilateral parahippocampal gyri, left hippocampus, bilateral anterior temporal poles, subgenual anterior cingulate, and orbitofrontal cortices (Figure 3, significant at cluster-level  $p < 0.05$  corrected). Cluster sizes and locations in terms of MNI coordinates for all significant clusters of association are listed in Table S2. Four ICNs influenced associations with these clusters, including the insulae, lat visual assoc, aTempPolar, and language networks (Figure 3, right, all connections significant at  $p < 0.05$ , corrected).

Gray matter volume was not associated with executive function composite scores in the VBM analysis (all clusters  $p > 0.05$ , corrected).

### 3.6 | Language

Language composite scores were primarily associated with premotor regions, including clusters in the left middle and superior frontal gyri, extending into the left supplementary motor area (Figure 4, significant at cluster-level  $p < 0.05$  corrected). Additional clusters were located

in the medial orbitofrontal, olfactory cortices, and the left cerebellum. Cluster sizes and locations in terms of MNI coordinates for all significant clusters of association are listed in Table S3.

Eleven ICNs influenced associations with these clusters (Figure 4, right, all connections significant at  $p < 0.05$ , corrected). The influences of somatomotor and associative sensory networks were prominent, including several somatomotor such as the L SM, R SM, and dSM. Additional influential sensory and motor networks

included the motor planning network, encompassing the pre-supplementary motor area, as well as auditory assoc, lat visual assoc and DAN. Influential limbic networks included the med temporal, insulae, and olfactory networks. Finally, the Putamen Network influenced associations with cerebellar and subgenual clusters.

Gray matter volume was not associated with language cognitive composite scores in the VBM analysis (all clusters  $p > 0.05$ , corrected).

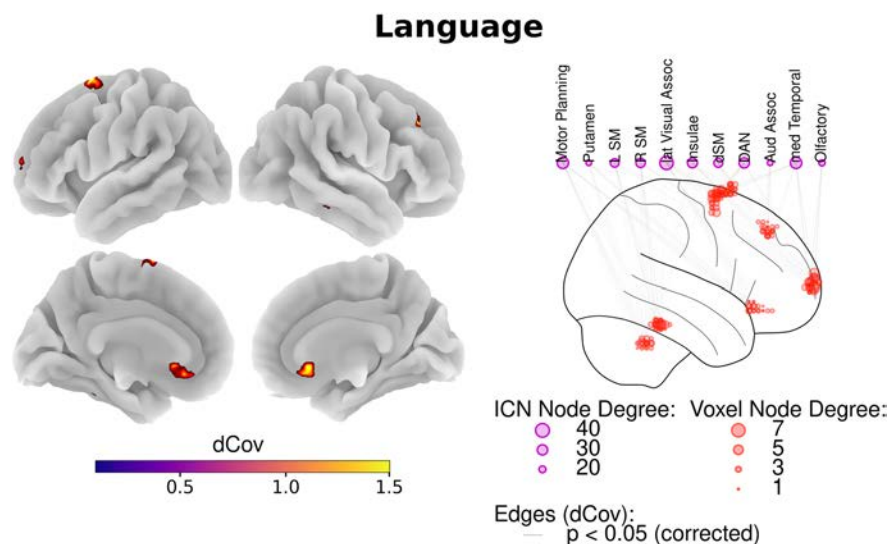


**FIGURE 4** Cortical and network associations with language. Left: Cortical associations displayed as surface renderings. As measured by distance covariance (dCov), language cognitive composite scores were associated with clusters in the left superior frontal gyrus, bilateral middle frontal gyrus, medial orbitofrontal and olfactory cortices, and left cerebellum (all clusters  $p < 0.05$ , corrected). Right: Intrinsic connectivity networks (ICNs) influencing cortical associations. Eleven ICNs influenced associations with language scores, including left and right and dorsal subdivisions of the somatomotor network, (L SM, R SM, and dSM, respectively), lateral visual association (lat Visual Assoc), the dorsal attention (DAN), auditory association (aud assoc), and medial temporal (med temporal) networks (all connections  $p < 0.05$ , corrected).

### Learning and Memory

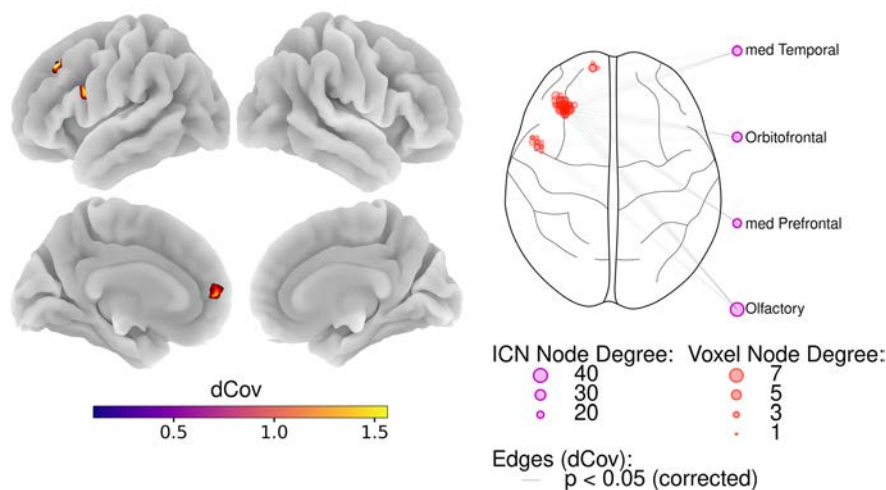


**FIGURE 5** Cortical and network associations with learning and memory. Left: Cortical associations displayed as surface renderings. As measured by distance covariance (dCov), learning and memory were associated with clusters in the left middle and superior frontal gyri and the medial prefrontal cortex (all clusters  $p < 0.05$ , corrected). Right: Intrinsic connectivity networks (ICNs) influencing cortical associations. Four ICNs influenced associations with learning and memory scores, including the medial temporal (med temporal), orbitofrontal, medial prefrontal (med prefrontal), and olfactory networks (all connections  $p < 0.05$ , corrected).

### 3.7 | Learning and memory

Learning and memory composite scores were associated with three clusters in the left prefrontal cortex, including the middle and superior frontal gyri and the medial prefrontal cortex (Figure 5, significant at cluster-level  $p < 0.05$  corrected; Table S4). Four networks influenced associations with these clusters, including the Orbitofrontal, med Temporal, Medial Prefrontal (med Prefrontal), and Olfactory networks (Figure 5, right, all connections significant at  $p < 0.05$ , corrected). Gray matter volume was not associated with learning and memory composite scores in the VBM analysis (all clusters  $p > 0.05$ , corrected).

### 3.8 | Visuospatial

Visuospatial scores were associated with connectivity involving a cluster in the left lingual gyrus along the calcarine sulcus, and a cluster in the right fusiform gyri that extended into the parahippocampal gyrus (Figure 6, left, significant at cluster-level  $p < 0.05$  corrected; Table S5). The bilateral caudate and precuneus (PrC) networks influenced associations with the left lingual gyrus, while the L SM influenced associations with the right fusiform cluster (Figure S4).

Gray matter volume in many cortical and subcortical regions were associated with visuospatial scores (Figure 6, right, significant at cluster-level  $p < 0.05$  corrected). Clusters of increased gray matter in the bilateral

pre-central gyri, bilateral opercula, right middle temporal gyrus, left superior temporal gyrus, and medial cerebellum were associated with increased visuospatial scores (Table S6).

### 3.9 | Global cognition

Global cognition composite scores were associated with a cluster in the left superior thalamus, as well as a cluster in the right cerebellum ( $x = -18$ ,  $y = -28$ ,  $z = 14$ ,  $k = 27$  voxels; significant at cluster-level  $p < 0.05$  corrected; Figure S5, Table S7). Associations with the right cerebellar cluster were influenced by connectivity to the L SM and L dlPFC networks. Connectivity involving four ICNs influenced associations with the left thalamic cluster, including the putamen, R dlPFC, L dlPFC, and motor planning networks. Gray matter volume was not associated with global cognition composite scores in the VBM analysis (all clusters  $p > 0.05$ , corrected).

## 4 | DISCUSSION

As hypothesized, cognitive measures in PD were associated with connectivity involving the hippocampus and basal ganglia. Additionally, beyond these hypothesized regions, associations were observed for cortical regions. The hypothesized associations were most evident for executive function composite scores, where connectivity involving subcortical and paralimbic regions influenced

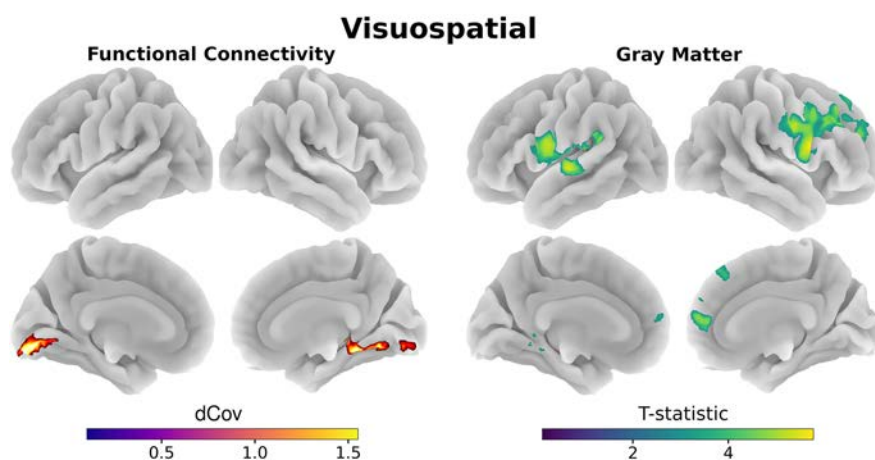


**FIGURE 6** Functional and structural cortical associations with visuospatial processing. Left: Cortical associations with functional connectivity displayed as surface renderings, measured by distance covariance (dCov). Connectivity was associated with visuospatial scores in the left lingual gyrus along the calcarine sulcus and the right fusiform gyri (all clusters  $p < 0.05$ , corrected). Right: Cortical associations with gray matter volumes, measured by voxel-based morphometry. Visuospatial scores were associated with gray matter volume in the bilateral pre-central gyri, bilateral operculum, right middle temporal gyrus, left superior temporal gyrus, and medial cerebellum (all clusters  $p < 0.05$ , corrected).

cognitive composite scores. In addition, other cognitive domains were associated with networks encompassing these subcortical regions. These included influences of the bilateral Putamen Network on attention, language and global cognition composite scores, the influence of the Caudate Network on visuospatial scores, and the influence of the Medial Temporal Network on associations with language, learning and memory composite scores. These results suggest that disease-associated pathology in these subcortical regions may lead to widespread dysfunctional cortical connectivity and the cognitive impairments associated with PD.

In healthy elderly subjects, total cortical atrophy is associated with cognitive decline resulting from normal aging (Chee et al., 2009; Fjell & Walhovd, 2010; Kramer et al., 2007; Van Petten et al., 2004). However, atrophy in specific regions such as the dlPFC, and its contributions to individual cognitive domains such as executive function, remain an open question in this population. Reports of specific structure-cognition associations in the absence of pathology are inconsistent and weakly supported by evidence (Fjell & Walhovd, 2010; Raz & Rodrigue, 2006; Salthouse, 2011). Contributing to this inconsistency are reports of counterintuitive negative correlations between regional gray matter volume and cognitive performance (Duarte et al., 2006; Salat et al., 2002; Van Petten et al., 2004). These results may suggest structure-cognition associations reflect pre-existing differences from earlier stages in the lifespan, such as synaptic pruning, rather than purely later age-related cognitive decline.

In neuropsychiatric patients, atrophy in specific regions is frequently associated with cognitive functions. In patients with Alzheimer's disease or vascular mild cognitive impairment, frontal gray matter volume correlates with executive function (Duarte et al., 2006; Lei et al., 2016). In patients with mild cognitive impairment, visuospatial deficits are associated with frontotemporal atrophy (Mitolo et al., 2013). Similar associations between visuospatial deficits and atrophy have been observed in a broad sample including patients with Alzheimer's disease, mild cognitive impairment, and healthy controls (Amaefule et al., 2021). In PD-MCI, visuospatial deficits have been associated with both frontal and parietotemporal atrophy (Garcia-Diaz et al., 2018; Lee et al., 2014; Segura et al., 2014).

In the current investigation gray matter atrophy was not generally associated with cognitive variability in PD, with the notable exception of visuospatial scores. These results suggest that functional connectivity may be a more sensitive marker of neuropathology associated with cognitive changes in PD. Furthermore, while both functional connectivity and VBM can link cognitive domains to specific regions within the brain, functional

connectivity potentially provides additional information about the dysfunctional processing associated with these deficits. For example, in the current investigation, connectivity to and from specific large-scale networks and the hippocampus and putamen contribute to specific cognitive impairments in PD.

Visuospatial associations with gray matter volume differed from associations with functional connectivity. While functional connectivity results were localized to the primary visual cortex and fusiform gyrus, gray matter volume was associated with primary sensory and motor cortices as well as with anterior (temporal and frontal) regions. In this case, the connectivity results appeared to reflect the disrupted visual processing evident in neuropsychological testing results in combination with underlying basal ganglia pathology in patients with PD (Emre, 2003a). Abnormal BOLD activity in visual networks in subjects with PD and cognitive impairments has been recently reported (Guo et al., 2021), suggesting a relationship between visual system alterations and cognition in PD. Interestingly, we did not observe an association between gray matter atrophy in posterior regions and visuospatial scores, previously reported with cortical thinning measures (Garcia-Diaz et al., 2018; Segura et al., 2014). However, because similar associations between visuospatial scores, temporoparietal, and frontal cortices were reported in early PD (Pereira et al., 2014), current results suggest that gray matter loss may progress to posterior regions along with decline in visuospatial ability.

Attention cognitive composite associations in PD followed the proposed dual attention systems within the brain (Corbetta & Shulman, 2002). The DAN exerted widespread influence on many regions, suggesting goal-directed and top-down influences on these cognitive measures. Acting in tandem with the DAN, the stimulus-driven Ventral Attention System encompasses right-lateralized frontoparietal regions such as the right inferior and middle frontal gyri. In the current results, associations between attention scores and predominantly right lateralized clusters in the inferior and middle frontal gyri may reflect influences of this system. Interactions between these clusters and the DAN may suggest an interplay between goal-driven and stimulus-driven directing of external attention as needed during cognitive testing, consistent with the proposed roles of these systems (Corbetta & Shulman, 2002).

Language cognitive composite scores were associated with clusters in premotor areas, such as the superior and medial frontal gyri. Similarly, language composite scores were influenced by connectivity involving the motor planning and insulae networks, in addition to subdivisions of the SM. These results are consistent with regions

activated during verbal fluency tasks in healthy controls (Corbetta & Shulman, 2002) and may reflect difficulties in the initiation and maintenance of attentional resources required during the cognitive tests.

Three gray matter regions were prominent in both the neuroanatomical and network levels of the analysis, namely the putamen, the hippocampus, and the olfactory cortex. Associations between connectivity involving the basal ganglia and hippocampus and executive function in PD is consistent with our hypothesis as well as the proposed broader primary and progressive pathology associated with the disease (Braak et al., 2003; Goedert et al., 2013). Similarly, the olfactory bulb is an early site of synuclein inclusions, with spread into the adjacent subgenual anterior cingulate as the disease progresses (Vogt, 2019). Interestingly, and consistent with the current results, abnormal activation in the hippocampus in PD patients has been associated with executive function task performance, even in patients without cognitive symptoms at baseline (Dagher et al., 2001). In contrast, hippocampal atrophy seems to be found in later stages of the disease (Christopher & Strafella, 2013; Delgado-Alvarado et al., 2016; Nagano-Saito et al., 2005). Given that executive function deficits are observed in early PD-MCI patients, hippocampal abnormalities could be early markers of disease progression. Decreased dopamine synthesis in the putamen of people with PD (Kish et al., 1988) is associated with performance deficits on tests of executive function, suggesting that dopamine depletion in this region impacts processing in frontostriatal circuits (Cropley et al., 2008), consistent with the connectivity results. Therefore, the associations between hippocampal and putamen connectivity with executive function, combined with non-significant associations between atrophy in the same regions and the same cognitive tests, suggest that disrupted hippocampal and putamen function and connectivity may be more prominent than atrophy in cognitive subgroups of PD.

Strengths of this study are its data-driven, holistic, fine-grained approach to analyzing cognitive associations using neuroimaging. These include a multidomain neurocognitive battery, voxel-level whole-brain analyses encompassing numerous large-scale networks, and comparison of structural and functional measures. The limitations of the current study include the lack of healthy comparison group and small sample size, precluding subgroup analyses including sex differences, as well as possible confounding effects from antiparkinsonian medications. Additionally, subjects may have had overlapping neurodegenerative disorders, such as PD and Alzheimer's disease. Future research directions include developing non-invasive neuroimaging tests to

investigate dysfunctional connectivity implicated in cognitive impairment in PD, as well as measuring Alzheimer's disease biomarkers in order to rule out the effects of overlapping clinical diagnoses.

## 5 | CONCLUSION

In summary, cognitive domain-associated neuropathology in PD patients was investigated using a combination of structural and functional neuroimaging. Gray matter atrophy, as measured using VBM, was associated with visuospatial impairments involving primary sensory and motor regions and networks. In contrast, functional connectivity, as measured using dCov and ICA, was associated with all cognitive domains, including attention and executive function, the primary cognitive domains impacted in PD. These results suggest that, in comparison to gray matter atrophy, functional connectivity may be more sensitive for investigating the neurobiology of cognitive phenotypes in PD. Performance on executive function cognitive tests was localized to connectivity involving the hippocampus and putamen. These results are consistent with the known pathophysiology of PD, and previous data-driven comprehensive investigations of dementia in PD.

## ACKNOWLEDGEMENTS

All phases of this study were supported by three National Institutes of Health grants 1K02NS080885-01A1 (PI: Kluger), 1R21NS093266-01A1 (PI: Kluger), and K01AT009894-01 (PI: Buard) and a Michael J. Fox Foundation for Parkinson's Research (Grant Number 10879; PI: Holden). The authors wish to thank Christine Martin, Sarah Rogers, and Abigail Simpson for their help with participant recruitment and neuropsychological testing administration.

## CONFLICT OF INTEREST

The author reports no conflicts of interest in this work.

## AUTHOR CONTRIBUTIONS

All authors have contributed to and approved the final manuscript. *Conceptualization*, K.P.W., B.M.K., and I.B.; *Methodology*, K.P.W., L.D.M., *Software*, K.P.W.; *Investigation*, K.P.W., L.D.M., S.K.H., E.K., I.B.; *Resources*, B.M.K., J.R.T., I.B.; *Writing -Original Draft*, K.P.W., I.B.; *Writing -Review & Editing*, B.M.K., L.D.M., S.K.H., E.K., J.R.T.; *Visualization*, K.P.W.; *Supervision*, B.M.K., I.B.

## PEER REVIEW

The peer review history for this article is available at <https://publons.com/publon/10.1111/ejn.15899>.

## DATA AVAILABILITY STATEMENT

The data that support the findings of this study are openly available in OpenNeuro at <https://openneuro.org/git/2/ds004392>, doi:10.18112/openneuro.ds004392.v1.0.0, reference number ds004392.

## ORCID

Korey P. Wylie  <https://orcid.org/0000-0003-1331-9611>

## REFERENCES

- Aarsland, D. (2016). Cognitive impairment in Parkinson's disease and dementia with Lewy bodies. *Parkinsonism & Related Disorders*, 22(Suppl 1), S144–S148. <https://doi.org/10.1016/j.parkreidis.2015.09.034>
- Amaefule, C. O., Dyrba, M., Wolfgruber, S., Polcher, A., Schneider, A., Fliessbach, K., Spottke, A., Meiberth, D., Preis, L., Peters, O., Incesoy, E. I., Spruth, E. J., Priller, J., Altenstein, S., Bartels, C., Wiltfang, J., Janowitz, D., Bürger, K., Laske, C., ... Teipel, S. J. (2021). Association between composite scores of domain-specific cognitive functions and regional patterns of atrophy and functional connectivity in the Alzheimer's disease spectrum. *NeuroImage Clinical*, 29, 102533. <https://doi.org/10.1016/j.nicl.2020.102533>
- Amboni, M., Tessitore, A., Esposito, F., Santangelo, G., Picillo, M., Vitale, C., Giordano, A., Erro, R., de Micco, R., Corbo, D., Tedeschi, G., & Barone, P. (2015). Resting-state functional connectivity associated with mild cognitive impairment in Parkinson's disease. *Journal of Neurology*, 262(2), 425–434. <https://doi.org/10.1007/s00415-014-7591-5>
- Ashburner, J. (2007). A fast diffeomorphic image registration algorithm. *NeuroImage*, 38(1), 95–113. <https://doi.org/10.1016/j.neuroimage.2007.07.007>
- Ashburner, J., & Friston, K. J. (2000). Voxel-based morphometry—The methods. *NeuroImage*, 11(6), 805–821. <https://doi.org/10.1006/nimg.2000.0582>
- Ashburner, J., & Friston, K. J. (2005). Unified segmentation. *NeuroImage*, 26(3), 839–851. <https://doi.org/10.1016/j.neuroimage.2005.02.018>
- Bell, A. J., & Sejnowski, T. J. (1995). An information-maximization approach to blind separation and blind deconvolution. *Neural Computation*, 7(6), 1129–1159. <https://doi.org/10.1162/neco.1995.7.6.1129>
- Braak, H., Tredici, K. D., Rüb, U., de Vos, R. A. I., Jansen Steur, E. N. H., & Braak, E. (2003). Staging of brain pathology related to sporadic Parkinson's disease. *Neurobiology of Aging*, 24(2), 197–211. [https://doi.org/10.1016/S0197-4580\(02\)00065-9](https://doi.org/10.1016/S0197-4580(02)00065-9)
- Buuren, S. V. (2018). *Flexible imputation of missing data* (Second edition, ed.). CRC Press, Taylor & Francis Group. <https://doi.org/10.1201/9780429492259>
- Calhoun, V. D., Adali, T., Pearlson, G. D., & Pekar, J. J. (2001). A method for making group inferences from functional MRI data using independent component analysis. *Human Brain Mapping*, 14(3), 140–151. <https://doi.org/10.1002/hbm.1048>
- Chee, M. W., Chen, K. H., Zheng, H., Chan, K. P., Isaac, V., Sim, S. K., Chuah, L. Y. M., Schuchinsky, M., Fischl, B., & Ng, T. P. (2009). Cognitive function and brain structure correlations in healthy elderly east Asians. *NeuroImage*, 46(1), 257–269. <https://doi.org/10.1016/j.neuroimage.2009.01.036>
- Christopher, L., & Strafella, A. P. (2013). Neuroimaging of brain changes associated with cognitive impairment in Parkinson's disease. *Journal of Neuropsychology*, 7(2), 225–240. <https://doi.org/10.1111/jnp.12015>
- Corbetta, M., & Shulman, G. L. (2002). Control of goal-directed and stimulus-driven attention in the brain. *Nature Reviews Neuroscience*, 3(3), 201–215. <https://doi.org/10.1038/nrn755>
- Cropley, V. L., Fujita, M., Bara-Jimenez, W., Brown, A. K., Zhang, X.-Y., Sangare, J., Herscovitch, P., Pike, V. W., Hallett, M., Nathan, P. J., & Innis, R. B. (2008). Pre- and post-synaptic dopamine imaging and its relation with frontostriatal cognitive function in Parkinson disease: PET studies with [<sup>11</sup>C]NNC 112 and [<sup>18</sup>F]FDOPA. *Psychiatry Research*, 163(2), 171–182. <https://doi.org/10.1016/j.psychres.2007.11.003>
- Dagher, A., Owen, A. M., Boecker, H., & Brooks, D. J. (2001). The role of the striatum and hippocampus in planning: A PET activation study in Parkinson's disease. *Brain: A Journal of Neurology*, 124(Pt 5), 1020–1032. <https://doi.org/10.1093/brain/124.5.1020>
- Delgado-Alvarado, M., Gago, B., Navalpotro-Gomez, I., Jiménez-Urbieta, H., & Rodriguez-Oroz, M. C. (2016). Biomarkers for dementia and mild cognitive impairment in Parkinson's disease. *Movement Disorders: Official Journal of the Movement Disorder Society*, 31(6), 861–881. <https://doi.org/10.1002/mds.26662>
- Dirnberger, G., & Jahanshahi, M. (2013). Executive dysfunction in Parkinson's disease: A review. *Journal of Neuropsychology*, 7(2), 193–224. <https://doi.org/10.1111/jnp.12028>
- Duarte, A., Hayasaka, S., Du, A., Schuff, N., Jahng, G. H., Kramer, J., Miller, B., & Weiner, M. (2006). Volumetric correlates of memory and executive function in normal elderly, mild cognitive impairment and Alzheimer's disease. *Neuroscience Letters*, 406(1–2), 60–65. <https://doi.org/10.1016/j.neulet.2006.07.029>
- Emre, M. (2003a). Dementia associated with Parkinson's disease. *The Lancet. Neurology*, 2(4), 229–237. [https://doi.org/10.1016/S1474-4422\(03\)00351-x](https://doi.org/10.1016/S1474-4422(03)00351-x)
- Emre, M. (2003b). What causes mental dysfunction in Parkinson's disease? *Movement Disorders: Official Journal of the Movement Disorder Society*, 18(Suppl 6), S63–S71. <https://doi.org/10.1002/mds.10565>
- Emre, M., Aarsland, D., Brown, R., Burn, D. J., Duyckaerts, C., Mizuno, Y., Broe, G. A., Cummings, J., Dickson, D. W., Gauthier, S., Goldman, J., Goetz, C., Korczyn, A., Lees, A., Levy, R., Litvan, I., McKeith, I., Olanow, W., Poewe, W., ... Dubois, B. (2007). Clinical diagnostic criteria for dementia associated with Parkinson's disease. *Movement Disorders: Official Journal of the Movement Disorder Society*, 22(12), 1689–1707. <https://doi.org/10.1002/mds.21507>
- Erhardt, E. B., Rachakonda, S., Bedrick, E., Allen, E., Adali, T., & Calhoun, V. D. (2011). Comparison of multi-subject ICA methods for analysis of fMRI data. *Human Brain Mapping*, 32(12), 2075–2095. <https://doi.org/10.1002/hbm.21170>
- Fischl, B. (2012). FreeSurfer. *NeuroImage*, 62(2), 774–781. <https://doi.org/10.1016/j.neuroimage.2012.01.021>
- Fischl, B., Sereno, M. I., Tootell, R. B., & Dale, A. M. (1999). High-resolution intersubject averaging and a coordinate system for the cortical surface. *Human Brain Mapping*, 8(4), 272–284.

- [https://doi.org/10.1002/\(sici\)1097-0193\(1999\)8:4<272::aid-hbm10>3.0.co;2-4](https://doi.org/10.1002/(sici)1097-0193(1999)8:4<272::aid-hbm10>3.0.co;2-4)
- Fjell, A. M., & Walhovd, K. B. (2010). Structural brain changes in aging: Courses, causes and cognitive consequences. *Reviews in the Neurosciences*, *21*(3), 187–221. <https://doi.org/10.1515/revneuro.2010.21.3.187>
- Gao, L.-L., & Wu, T. (2016). The study of brain functional connectivity in Parkinson's disease. *Translational Neurodegeneration*, *5*, 18. <https://doi.org/10.1186/s40035-016-0066-0>
- Garcia-Diaz, A. I., Segura, B., Baggio, H. C., Uribe, C., Campabadal, A., Abos, A., Marti, M. J., Valdeoriola, F., Compta, Y., Bargallo, N., & Junque, C. (2018). Cortical thinning correlates of changes in visuospatial and visuo-perceptual performance in Parkinson's disease: A 4-year follow-up. *Parkinsonism & Related Disorders*, *46*, 62–68. <https://doi.org/10.1016/j.parkreldis.2017.11.003>
- Goedert, M., Spillantini, M. G., Del Tredici, K., & Braak, H. (2013). 100 years of Lewy pathology. *Nature Reviews Neurology*, *9*(1), 13–24. <https://doi.org/10.1038/nrneuro.2012.242>
- Goldman, J. G., Holden, S., Bernard, B., Ouyang, B., Goetz, C. G., & Stebbins, G. T. (2013). Defining optimal cutoff scores for cognitive impairment using Movement Disorder Society Task Force criteria for mild cognitive impairment in Parkinson's disease. *Movement Disorders*, *28*(14), 1972–1979. <https://doi.org/10.1002/mds.25655>
- Guo, W., Jin, W., Li, N., Gao, J., Wang, J., Chang, Y., Yin, K., Chen, Y., Zhang, S., & Wang, T. (2021). Brain activity alterations in patients with Parkinson's disease with cognitive impairment based on resting-state functional MRI. *Neuroscience Letters*, *747*, 135672. <https://doi.org/10.1016/j.neulet.2021.135672>
- Hammers, A., Allom, R., Koeppe, M. J., Free, S. L., Myers, R., Lemieux, L., Mitchell, T. N., Brooks, D. J., & Duncan, J. S. (2003). Three-dimensional maximum probability atlas of the human brain, with particular reference to the temporal lobe. *Human Brain Mapping*, *19*(4), 224–247. <https://doi.org/10.1002/hbm.10123>
- Hanagasi, H. A., Tufekcioglu, Z., & Emre, M. (2017). Dementia in Parkinson's disease. *Journal of the Neurological Sciences*, *374*, 26–31. <https://doi.org/10.1016/j.jns.2017.01.012>
- Hohenfeld, C., Werner, C. J., & Reetz, K. (2018). Resting-state connectivity in neurodegenerative disorders: Is there potential for an imaging biomarker? *NeuroImage Clinica*, *18*, 849–870. <https://doi.org/10.1016/j.nicl.2018.03.013>
- Hua, W.-Y., & Ghosh, D. (2015). Equivalence of kernel machine regression and kernel distance covariance for multidimensional phenotype association studies. *Biometrics*, *71*(3), 812–820. <https://doi.org/10.1111/biom.12314>
- Hughes, A. J., Daniel, S. E., Kilford, L., & Lees, A. J. (1992). Accuracy of clinical diagnosis of idiopathic Parkinson's disease: A clinico-pathological study of 100 cases. *Journal of Neurology, Neurosurgery, and Psychiatry*, *55*(3), 181–184. <https://doi.org/10.1136/jnnp.55.3.181>
- Kalaitzakis, M. E., & Pearce, R. K. B. (2009). The morbid anatomy of dementia in Parkinson's disease. *Acta Neuropathologica*, *118*(5), 587–598. <https://doi.org/10.1007/s00401-009-0597-x>
- Kehagia, A. A., Barker, R. A., & Robbins, T. W. (2010). Neuropsychological and clinical heterogeneity of cognitive impairment and dementia in patients with Parkinson's disease. *The Lancet Neurology*, *9*(12), 1200–1213. [https://doi.org/10.1016/S1474-4422\(10\)70212-X](https://doi.org/10.1016/S1474-4422(10)70212-X)
- Kish, S. J., Shannak, K., & Hornykiewicz, O. (1988). Uneven pattern of dopamine loss in the striatum of patients with idiopathic Parkinson's disease. *New England Journal of Medicine*, *318*(14), 876–880. <https://doi.org/10.1056/NEJM198804073181402>
- Kramer, J. H., Mungas, D., Reed, B. R., Wetzell, M. E., Burnett, M. M., Miller, B. L., Weiner, M. W., & Chui, H. C. (2007). Longitudinal MRI and cognitive change in healthy elderly. *Neuropsychology*, *21*(4), 412–418. <https://doi.org/10.1037/0894-4105.21.4.412>
- Lee, J. E., Cho, K. H., Song, S. K., Kim, H. J., Lee, H. S., Sohn, Y. H., & Lee, P. H. (2014). Exploratory analysis of neuropsychological and neuroanatomical correlates of progressive mild cognitive impairment in Parkinson's disease. *Journal of Neurology, Neurosurgery, and Psychiatry*, *85*(1), 7–16. <https://doi.org/10.1136/jnnp-2013-305062>
- Lei, Y., Su, J., Guo, Q., Yang, H., Gu, Y., & Mao, Y. (2016). Regional gray matter atrophy in vascular mild cognitive impairment. *Journal of Stroke and Cerebrovascular Diseases*, *25*(1), 95–101. <https://doi.org/10.1016/j.jstrokecerebrovasdis.2015.08.041>
- Li, Y.-O., Adali, T., & Calhoun, V. D. (2007). Estimating the number of independent components for functional magnetic resonance imaging data. *Human Brain Mapping*, *28*(11), 1251–1266. <https://doi.org/10.1002/hbm.20359>
- Litvan, I., Goldman, J. G., Tröster, A. I., Schmand, B. A., Weintraub, D., Petersen, R. C., Mollenhauer, B., Adler, C. H., Marder, K., Williams-Gray, C. H., Aarsland, D., Kulisevsky, J., Rodriguez-Oroz, M. C., Burn, D. J., Barker, R. A., & Emre, M. (2012). Diagnostic criteria for mild cognitive impairment in Parkinson's disease: Movement Disorder Society Task Force guidelines. *Movement Disorders*, *27*(3), 349–356. <https://doi.org/10.1002/mds.24893>
- Mitolo, M., Gardini, S., Fasano, F., Crisi, G., Pelosi, A., Pazzaglia, F., & Caffarra, P. (2013). Visuospatial memory and neuroimaging correlates in mild cognitive impairment. *Journal of Alzheimer's Disease*, *35*(1), 75–90. <https://doi.org/10.3233/JAD-121288>
- Nagano-Saito, A., Washimi, Y., Arahata, Y., Kachi, T., Lerch, J. P., Evans, A. C., Dagher, A., & Ito, K. (2005). Cerebral atrophy and its relation to cognitive impairment in Parkinson disease. *Neurology*, *64*(2), 224–229. <https://doi.org/10.1212/01.WNL.0000149510.41793.50>
- Nakagawa, S., & Freckleton, R. P. (2008). Missing inaction: The dangers of ignoring missing data. *Trends in Ecology & Evolution*, *23*(11), 592–596. <https://doi.org/10.1016/j.tree.2008.06.014>
- Newman, M. (2010). *Networks: An introduction*. Oxford University Press. <https://doi.org/10.1093/acprof:oso/9780199206650.001.0001>
- Nichols, T. E., & Holmes, A. P. (2002). Nonparametric permutation tests for functional neuroimaging: A primer with examples. *Human Brain Mapping*, *15*(1), 1–25. <https://doi.org/10.1002/hbm.1058>
- Parkes, L., Fulcher, B., Yucesel, M., & Fornito, A. (2018). An evaluation of the efficacy, reliability, and sensitivity of motion correction strategies for resting-state functional MRI. *NeuroImage*, *171*, 415–436. <https://doi.org/10.1016/j.neuroimage.2017.12.073>

- Passingham, R. E., Stephan, K. E., & Kötter, R. (2002). The anatomical basis of functional localization in the cortex. *Nature Reviews Neuroscience*, 3(8), 606–616. <https://doi.org/10.1038/nrn893>
- Pereira, J. B., Svenningsson, P., Weintraub, D., Bronnick, K., Lebedev, A., Westman, E., & Aarsland, D. (2014). Initial cognitive decline is associated with cortical thinning in early Parkinson disease. *Neurology*, 82(22), 2017–2025. <https://doi.org/10.1212/WNL.0000000000000483>
- Power, J. D., Barnes, K. A., Snyder, A. Z., Schlaggar, B. L., & Petersen, S. E. (2012). Spurious but systematic correlations in functional connectivity MRI networks arise from subject motion. *NeuroImage*, 59(3), 2142–2154. <https://doi.org/10.1016/j.neuroimage.2011.10.018>
- Raz, N., & Rodrigue, K. M. (2006). Differential aging of the brain: Patterns, cognitive correlates and modifiers. *Neuroscience and Biobehavioral Reviews*, 30(6), 730–748. <https://doi.org/10.1016/j.neubiorev.2006.07.001>
- Salat, D. H., Kaye, J. A., & Janowsky, J. S. (2002). Greater orbital prefrontal volume selectively predicts worse working memory performance in older adults. *Cerebral Cortex*, 12(5), 494–505. <https://doi.org/10.1093/cercor/12.5.494>
- Salthouse, T. A. (2011). Neuroanatomical substrates of age-related cognitive decline. *Psychological Bulletin*, 137(5), 753–784. <https://doi.org/10.1037/a0023262>
- Segura, B., Baggio, H. C., Marti, M. J., Valldeoriola, F., Compta, Y., Garcia-Diaz, A. I., Vendrell, P., Bargallo, N., Tolosa, E., & Junque, C. (2014). Cortical thinning associated with mild cognitive impairment in Parkinson's disease. *Movement Disorders*, 29(12), 1495–1503. <https://doi.org/10.1002/mds.25982>
- Seibert, T. M., Murphy, E. A., Kaestner, E. J., & Brewer, J. B. (2012). Interregional correlations in Parkinson disease and Parkinson-related dementia with resting functional MR imaging. *Radiology*, 263(1), 226–234. <https://doi.org/10.1148/radiol.12111280>
- Sejdinovic, D., Sriperumbudur, B., Gretton, A., & Fukumizu, K. (2013). Equivalence of distance-based and RKHS-based statistics in hypothesis testing. *The Annals of Statistics*, 41, 2263–2291. <https://doi.org/10.1214/13-AOS1140>
- Shirer, W. R., Ryali, S., Rykhlevskaia, E., Menon, V., & Greicius, M. D. (2012). Decoding subject-driven cognitive states with whole-brain connectivity patterns. *Cerebral Cortex*, 22(1), 158–165. <https://doi.org/10.1093/cercor/bhr099>
- Simon, N., & Tibshirani, R. (2014). Comment on “detecting novel associations in large data sets” by reshef et al, science dec 16, 2011. *arXiv preprint arXiv:1401.7645*.
- Stefanis, L. (2012).  $\alpha$ -Synuclein in Parkinson's disease. *Cold Spring Harbor Perspectives in Medicine*, 2(2), a009399. <https://doi.org/10.1101/cshperspect.a009399>
- Székely, G. J., Rizzo, M. L., & Bakirov, N. K. (2007). Measuring and testing dependence by correlation of distances. *Annals of Statistics*, 35(6), 2769–2794. <https://doi.org/10.1214/009053607000000505>
- Van Petten, C., Plante, E., Davidson, P. S., Kuo, T. Y., Bajuscak, L., & Glisky, E. L. (2004). Memory and executive function in older adults: Relationships with temporal and prefrontal gray matter volumes and white matter hyperintensities. *Neuropsychologia*, 42(10), 1313–1335. <https://doi.org/10.1016/j.neuropsychologia.2004.02.009>
- Vogt, B. A. (2019). Cingulate cortex in Parkinson's disease. In *Handbook of clinical neurology* (Vol. 166) (pp. 253–266). Elsevier.
- Yeo, B. T. T., Krienen, F. M., Sepulcre, J., Sabuncu, M. R., Lashkari, D., Hollinshead, M., Roffman, J. L., Smoller, J. W., Zöllei, L., Polimeni, J. R., Fischl, B., Liu, H., & Buckner, R. L. (2011). The organization of the human cerebral cortex estimated by intrinsic functional connectivity. *Journal of Neurophysiology*, 106(3), 1125–1165. <https://doi.org/10.1152/jn.00338.2011>
- Zigmond, A. S., & Snaith, R. P. (1983). The hospital anxiety and depression scale. *Acta Psychiatrica Scandinavica*, 67(6), 361–370. <https://doi.org/10.1111/j.1600-0447.1983.tb09716.x>

## SUPPORTING INFORMATION

Additional supporting information can be found online in the Supporting Information section at the end of this article.

**How to cite this article:** Wylie, K. P., Kluger, B. M., Medina, L. D., Holden, S. K., Kronberg, E., Tregellas, J. R., & Buard, I. (2023). Hippocampal, basal ganglia and olfactory connectivity contribute to cognitive impairments in Parkinson's disease. *European Journal of Neuroscience*, 57(3), 511–526. <https://doi.org/10.1111/ejn.15899>